p. 頸動脈超音波：動脈硬化性疾患の早期発見ツールとして

長束一行（国立循環器病研究センター脳神経内科）

Introduction

頸動脈超音波検査は，簡便で，非侵襲であり，動脈硬化のスクリーニング検査として普及してきている。ごく初期の動脈硬化から高度な動脈硬化まで幅広く評価が可能で，全身の動脈硬化のサロゲートマーカーとして，多くの研究でも用いられている。

当院では冠動脈バイパス術に際して，スクリーニング検査として頸動脈エコー検査を実施しているが，30%程度に有意狭窄が見つかる。また逆に頸動脈狭窄で血行再建術をする際に，冠動脈のスクリーニング検査を行うと高率に冠動脈病変が見つかる。当院の予防検診部では疫学調査の検査項目として長期間頸動脈エコー検査を実施して追跡調査を行っているが，日本人でも内膜中膜厚（intima media thickness；IMT）が心血管疾患の独立した危険因子であることがわかった。

注意点としては，超音波検査は術者による技量の差があり再現性を保つためにはできるだけ自動計測で定量化を行っていくことが理想であるが，まだ普及していないこと，そしてまだ統一された計測法のガイドラインがないことがあげられる。

頸動脈超音波検査装置

まず超音波診断装置であるが，この10年ほどの間の進歩は著しく，当然新しい機器のほうが簡単できれいな描出が可能である。機能としてはデュプレックスドプラ（図1）とよばれる，sampling pointを設定して血流速度を測る機能，カラードプラは最低限必要である。

探触子は基本的には7MHz以上の高周波数のリニアプローブが1本あればよいが，余裕があれば5MHz程度のミニコンベックスとよばれるプローブがあれば，血管が深い位置にある場合役立つ。また遅い血流や，逆に狭窄部の早い血流が血管外にはみ出しにくい，dynamic flowやB flow（図2）のような機能があると便利である。

頸動脈超音波検査の手順

決まった方法はないが，一定の手順

1. 超音波

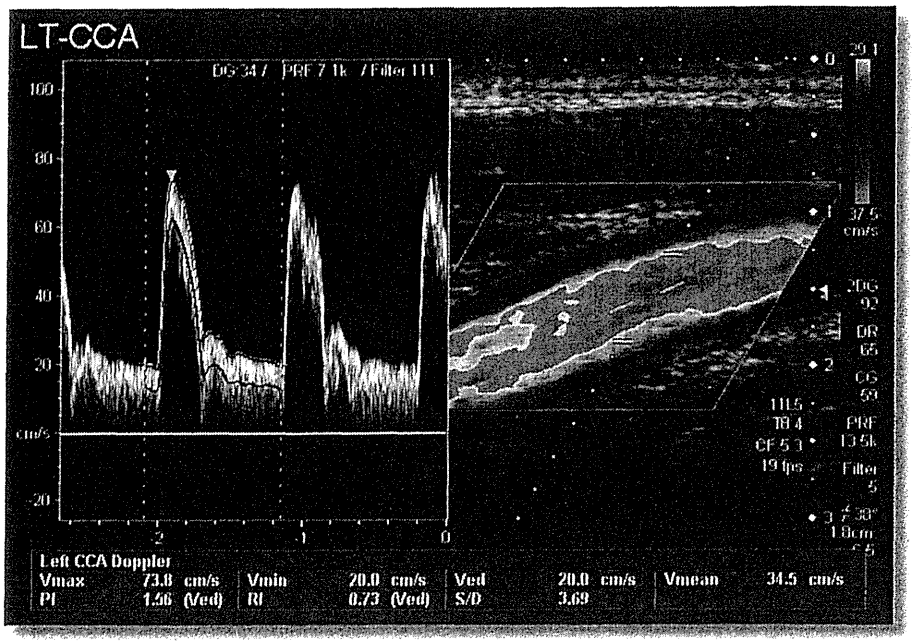

図1 デュプレックスドプラによる血流速度計測

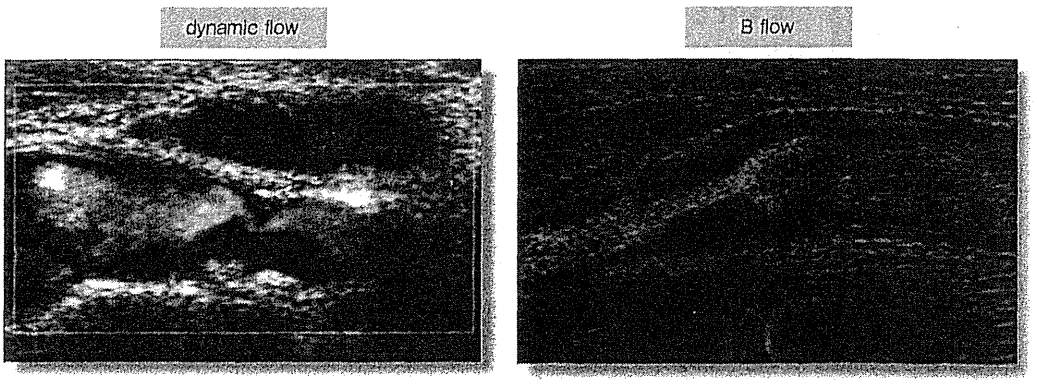

図2 高度狭窄部の描出に優れる新技術

を踏んだほうが見逃しが少ない。筆者らの施設では，基本は被験者を臥位にし，枕をはずして検査する側の反対側に軽く顔を傾け検査にかかる。

(1)短軸でのスキャン

まず短軸のBモード像で総頸動脈を描出し，できるだけ総頸動脈の心臓側遠位部から分岐部，内頸動脈，外頸動脈をできるだけ頭側まで見える範囲で広くスキャンする。このときにプラークの有無や血管の走行をチェックしておく。

もう一度カラードプラをオンにして，短軸での操作を行い，低輝度プラークの見逃しがないかをチェックする。ただし短軸でカラーイメージが欠損しているからといって，その部位を直ちに低輝度プラークと判断してはならない。特に分岐部では血流が乱流になったり，流速が遅くなる部分があるのでその部分が欠損像として表れ

る。短軸では特に影響を受けやすいので，カラードプラで欠損部が見つかれば，長軸にして血管に角度を付け，繰り返し周波数を落としたり，カラーゲインを上げて本当に低輝度プラークがあるのかを慎重に確認する必要がある(図3)。

(2) IMT計測

短軸でのスキャンが終われば，内中膜を長軸で描出して，IMTを計測する(図4)。IMTの計測部位も決まった統一された方法はなく，少なくとも現時点では総頸動脈，分岐部，内頸動脈のプラークを含めて最も肥厚した部分をmaxIMTとして計測しておくとよい。また理論上は近位壁(near wall)よりも遠位壁(far wall)のほうが検出感度も精度も高い。

内中膜描出の際，よくみかける注意点として，血管の走行をプローブとなるべく平行にして描出，計測することがポイントである。Bモード画像は，超音波信号が対象物に直角にあたったときに最も正確な画像が得られる。

(3) 血流速度の計測

続いて，総頸動脈，内頸動脈，外頸動脈の血流速度を計測する。狭窄部があれば必ず狭窄直後の収縮期最高血流速度(peak systolic velocity；PSV)を計測しておく。PSVが2m/secを超えればNASCETで70%以上の狭窄が存在する。またNASCET 50%狭窄のPSVはいろいろな報告があるが，頸動脈超音波検査はスクリーニング検査であるので閾値を下げて，見逃しを減らすほうがよいと考えられ，130cm/secを閾値と考えている。

最後に可能であれば椎骨動脈の描出と，血流速度の計測もできるようにしておいたほうがよい。

椎骨動脈の狭窄や閉塞に関しては図5のフローチャートが用いられてい

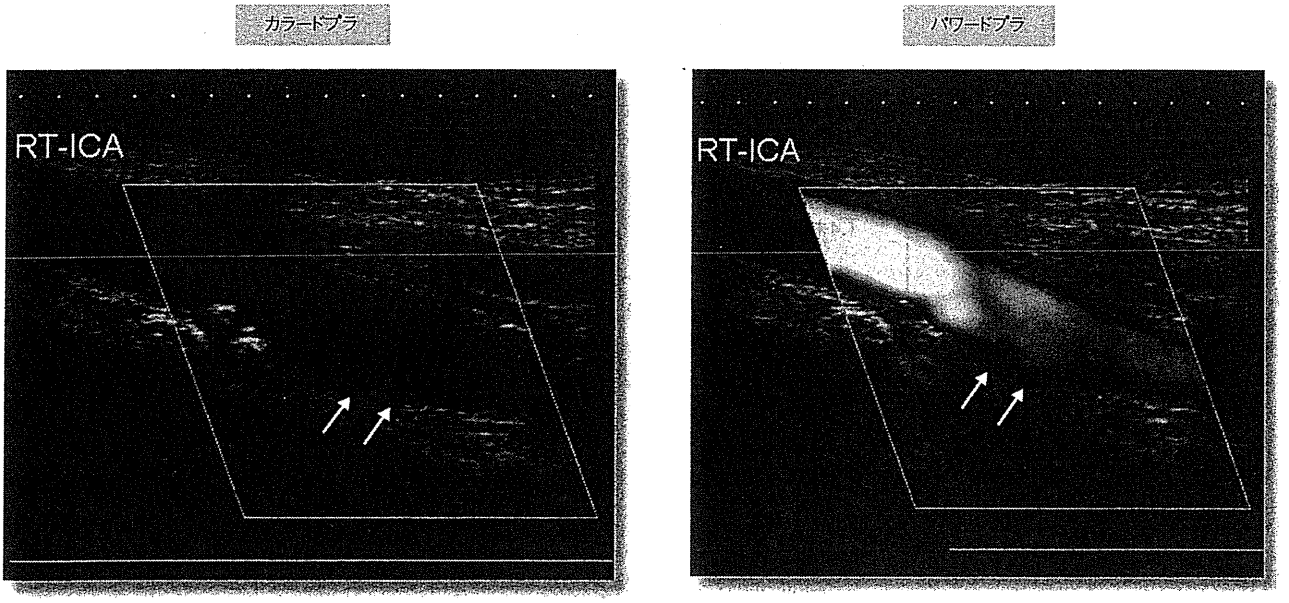

図3 分岐部でよく間違われるカラードプラの陰影欠損
繰り返し周波数を下げたり，パワードプラを用いることでこの陰影欠損部が低輝度プラークではないことがわかる。

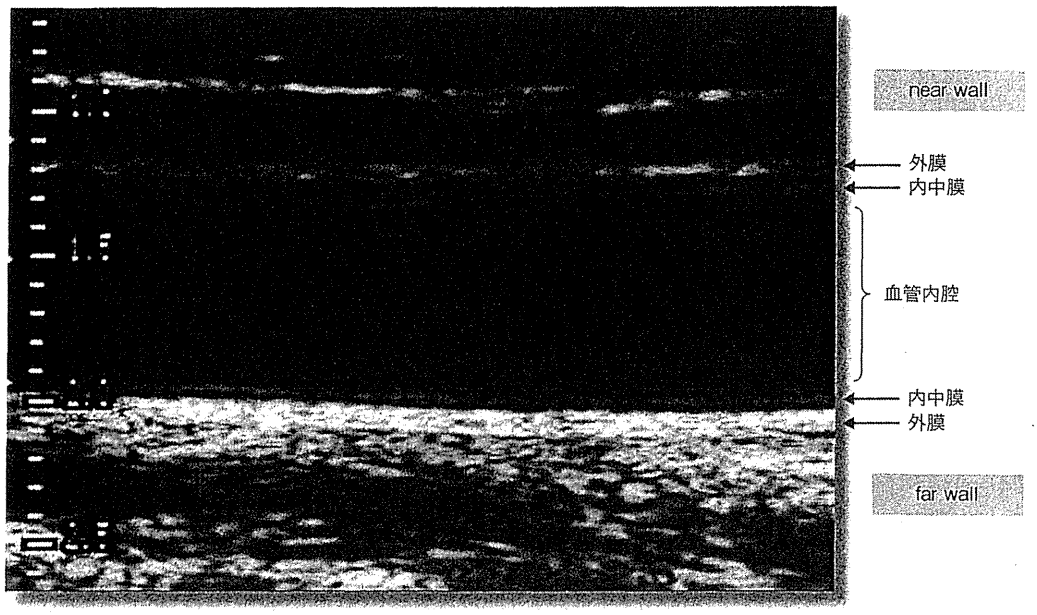

図4 総頸動脈でのIMT

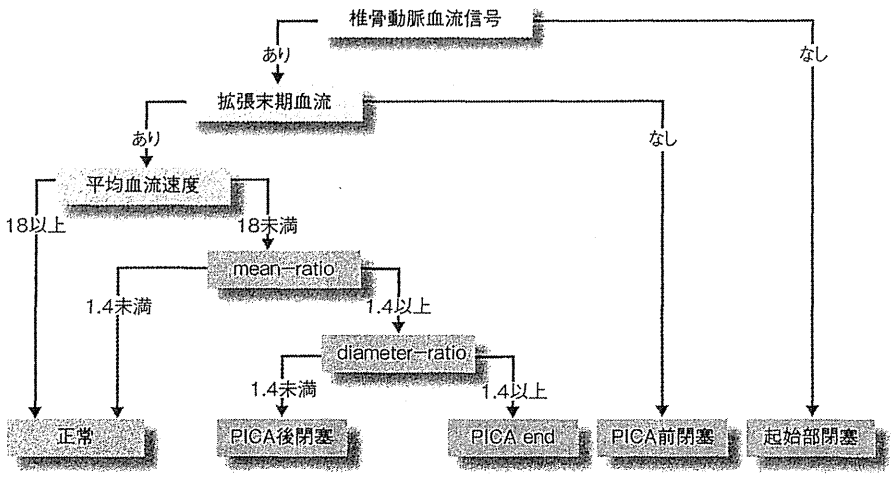

図5 椎骨動脈病変の診断フローチャート

PICA endは先天的に椎骨動脈に左右差があり，細い側の椎骨動脈がPICA(後下小脳動脈)を出した後，脳底動脈とつながっていない状態を示し，病的ではないと判断する。

る。椎骨動脈狭窄の好発部位の1つは起始部であるが，起始部の狭窄は直後の血流速度を計測することが診断に重要である。

動脈硬化性疾患と頸動脈超音波検査の関連

頸動脈超音波検査所見と動脈硬化性疾患に関しては，これまでに多数の報告がある。そのなかで最も多く使われている超音波所見はIMTである。

IMTは動脈硬化性疾患で肥厚して

おり，さらに将来の心血管疾患の独立した予測因子でもある[1]。ただしIMTの肥厚した症例に対して全例で冠動脈CTを施行するなどということは非常識であり，選択基準や，検査の進め方を考慮すべきである。

残念ながらIMTの肥厚がどの程度であれば，どこまで次の検査をすべきかというガイドラインはない。またIMTの正常値も年齢により変化するため，どこからを異常とするのかについても議論が分かれる。現状では年齢，性別，リスクファクター，心電図所見を参考に，リスクが高ければ心エコー，負荷心電図というように検査を進めていっている。逆にIMTが肥厚していないから冠動脈病変が絶対に存在していないわけではないので，あくまでも確率が高いということが証明されているのみであることを理解しておく必要がある。

またIMTによる研究から高血圧，糖尿病，脂質異常症，年齢，性差などの古典的な危険因子のほかに，慢性炎症（歯周病や慢性肝炎など），睡眠時無呼吸[2]などさまざまな多因性の要素が見つかり，10歳の子供のころからすでに肥満しているほうがIMTが有意に肥厚しているという驚くべき報告もなされている[3]。

介入試験のサロゲートエンドマーカーとしても多くの薬剤でIMTが薄くなったり，肥厚の進展が抑制されるなどの報告が次々に報告されてきており，薬物治療により動脈硬化を退縮させることが可能であると考えられトピックスとなった[4]。

これまで海外の疫学調査でIMTが循環器疾患の独立した予測因子であることが報告されてきたが，今後は個人の経時的変化が介入によりどのように変化するのか，イベント発症との関連を明らかにしていくことが重要である。しかし現時点でこれらの因果関係を明確に示せた報告はない。

個人の経時的変化をとらえるためには，再現性を高くし，精度も上げる必要がある。少なくとも1点の手動での計測では不可能と考えられ，自動計測で測定位置に関しても繰り返し同じ範囲を同じ方向から計測できる装置の工夫が必要である。IMT計測部位や方法，プラークの定義すらまだ日本で統一した基準ができておらず，今後の課題と考えている。

■ 文献

1) O'Leary DH, Polak JF, Kronmal RA, et al; Carotid-artery intima and media thickness as a risk factor for myocardial infarction and stroke in older adults. Cardiovascular health study collaborative research group. N Engl J Med 340: 14-22, 1999.
2) Kaynak D, Goksan B, Kaynak H, et al: Is there a link between the severity of sleep-disordered breathing and atherosclerotic disease of the carotid arteries? Eur J Neurol 10: 487-493, 2003.
3) Jarvisalo MJ, Harmoinen A, Hakanen M, et al: Elevated serum c-reactive protein levels and early arterial changes in healthy children. Arterioscler Thromb Vasc Biol 22: 1323-1328, 2002.
4) Smilde TJ, van Wissen S, Wollersheim H, et al: Effect of aggressive versus conventional lipid lowering on atherosclerosis progression in familial hypercholesterolaemia (asap): A prospective, randomised, double-blind trial. Lancet 357: 577-581, 2001.

Upregulation of ANGPTL4 Messenger RNA and Protein in Severely Calcified Carotid Plaques

Hiroyuki Katano, MD, PhD,*† and Kazuo Yamada, MD, PhD*

Background: In carotid atherosclerotic lesions, calcified plaques are thought to be stable and to evoke very few symptoms. However, the molecular activity in calcified plaques and their clinical significance have not been fully clarified yet. *Methods:* Carotid plaques from 18 endarterectomy patients were classified into high- and low-calcified plaques on the basis of Agatston calcium score. Twelve plaques were investigated for the alteration of gene expression by microarray analysis and real-time polymerase chain reaction (PCR) and 6 other plaques underwent protein assessment to elucidate the difference in molecular biological activity between the groups. *Results:* Microarray analysis demonstrated 93 angiogenesis or growth factor–related transcripts that are reliably expressed (175 probe sets). Among them, angiopoietin-like protein 4 (ANGPTL4) expression was significantly elevated, whereas fibroblast growth factor receptor 2 (FGFR2) expression was significantly suppressed. Quantitative messenger RNA analysis was performed with real-time PCR. Augmented or decreased protein expression of each gene was confirmed by Western blotting analysis and immunohistochemistry. *Conclusions:* In high-calcified plaques, ANGPTL4 might be upregulated for antiangiogenic modulating function together with the downregulation of FGFR2, contributing to the stability of the plaques. **Key Words:** Carotid plaque—calcification—microarray analysis—ANGPTL4—FGFR2—angiogenesis.

Introduction

The mechanism of vascular calcification formation and its clinical significance have not been fully clarified yet. Calcification has been thought to be a terminal state of the tissue in the pathological course of atherosclerosis that ended up in necrosis or apoptosis. Apoptotic bodies derived from vascular smooth muscle cells have been reported to serve as a nidus for calcification.[1] Lipoprotein such as acetylated low-density lipoprotein in atherosclerotic plaque was found to prevent phagocytosis of vascular-derived apoptotic vesicles that would otherwise serve as a core of calcification.[2] In carotid atherosclerotic lesions, calcified plaques were, hence, thought to be stable and hardly evoke symptoms, whereas unstable deleterious plaques were reported to be so-called "soft," hemorrhagic, or mobile plaques.[3] Nandalur et al[4] reported that plaque calcification of more than 45% of the total volume was significantly inversely associated with the occurrence of symptoms, whereas Kwee[5] found through a systematic review that clinically symptomatic plaques have a lower degree of calcification than asymptomatic plaques.

We planned, therefore, to classify the carotid plaques into high- and low-calcified plaques on the basis of

From the *Department of Neurosurgery, Nagoya City University Graduate School of Medical Sciences, Nagoya; and †Department of Medical informatics and Integrative Medicine, Nagoya City University Graduate School of Medical Sciences, Nagoya, Japan.

Received April 3, 2013; revision received July 27, 2013; accepted July 31, 2013.

Funding: This work was supported by JSPS KAKENHI (grant number 23592102).

Conflict of interests: The authors declared no conflicts of interest with respect to the authorship and/or publication of this article.

Address correspondence to Hiroyuki Katano, MD, Department of Neurosurgery, Nagoya City University Graduate School of Medical Sciences, 1 Kawasumi, Mizuho-cho, Mizuho-ku, Nagoya 467-8601, Japan. E-mail: katano@med.nagoya-cu.ac.jp.

1052-3057/$ - see front matter

http://dx.doi.org/10.1016/j.jstrokecerebrovasdis.2013.07.046

Agatston calcium score and investigate the alteration of gene expression by microarray analysis followed by protein assessment to elucidate the difference in molecular biological activity between the groups.

Materials and Methods

Patients and Specimens

Carotid plaques from 18 endarterectomy patients were investigated. Of these, 12 plaques were used for the gene expression analysis and another 6 plaques were used for Western blotting and immunohistochemistry. In each group, half of the plaques were highly calcified plaques that showed a mean calcium score of 839.9 ± 569.0, whereas the rest of the low-calcified plaques showed a mean calcium score of 52.5 ± 36.7. Macroscopic hemorrhages and ulcers were more frequently found in the low-calcified plaques than the high-calcified ones. The percentage of symptomatic cases was the same (77.8%) in both groups, and there were no significant differences in the degrees of stenoses between the groups (83.8% ± 11.0% versus 80.6% ± 6.2%). No remarkable difference was found between high- and low-calcified plaques concerning clinical data except hypertension and smoking habit (Table 1).

All patients enrolled in this study received a detailed explanation on the nature of the project, and all gave written informed consent before undergoing endarterectomy. Approval of the local ethical committee for human genetic research was also obtained before the start of the study. The patients underwent preoperative multidetector computed tomography angiography (MDCTA) that identified the plaque location and the degree of stenosis. Evaluation of calcification of the plaques using Agatston calcium score was also performed using MDCTA as described previously.[6] Briefly, calcification of the carotid plaque was quantified using specialized software run on the workstation (Aquarious; TeraRecon, Inc., San Mateo, CA) with preoperative MDCTA data. Calcium scores were calculated as the products of the areas of calcified lesions and the weighted signal intensity scalars, dependent on the maximal Hounsfield unit value within the lesion (scalar = 1 if 130-199, 2 if 200-299, 3 if 300-399, and 4 if 400 Hounsfield units or greater). All carotid plaques were obtained during carotid endarterectomy, and whole specimens containing a calcified portion were immediately treated with RNA later (Ambion, Austin, TX). All samples were stored at −80°C and thawed only once.

Microarray

The methods used for sample preparation, hybridization, data analysis, sensitivity, and quantification are based on the Affymetrix GeneChip Expression Analysis Manual (Affymetrix, Santa Clara, CA). We used Affymetrix Human Genome U133 Plus 2.0 Array containing more than 54,000 probe sets representing 47,400 transcripts derived from 38,500 well-substantiated human genes and expressed sequence tags (unknown genes).

Total RNA was extracted from each plaque sample, cleaned, and converted to double-stranded complementary DNA (cDNA) and then to biotin-labeled complementary RNA according to the manufacturer's protocols. After quality confirmation with an Agilent 2100 Bioanalyzer (Aligent Technologies, Santa Clara, CA), biotinylated complementary RNA was hybridized to the Affymetrix Human Genome U133 Plus 2.0 chips. Hybridization of each chip was performed with the Hybridization, Wash, and Stain Kit according to GeneChip 3'IVT Express Kit User Manual and scanned with a probe array scanner. GeneChip raw data were obtained with Affymetrix GeneChip Command Console Software. After the mean value for the signal of each chip was normalized and scaled using the Micro Array Suite 5 statistical algorithm with Affymetrix Expression Console Software, analysis of the expression ratio comparing low and highly calcified groups was performed. Processed gene expression data were returned in a log2 scale. We compared 7 sets of high- and low-calcified plaques: set A: H1/L1, B: H2/L1, C: H3/L1, D: H1/L2, E: H2/L2, F: H3/L2, and G: H1/L3. Genes expressed at a reliable level and showing differential expression were identified by filtering. Detection calls were classified as present (P; transcripts detected), absent (A; transcripts not detected), or marginal (M; difficult to judge whether P or A). A transcript was considered differentially expressed if it satisfied the either following criteria: (1) (log2 ratio ≥ 1 and the detection call of the highly calcified plaque "P") in more than 5 of 7 comparison sets or (2) (log2 ratio ≤ −1 and the detection call of the low-calcified plaque "P") in more than 5 of 7 comparison sets. Among all the expressed transcripts by GeneChip analysis, angiogenesis or growth factor–related, calcification or osteogenesis-related and hypoxia-inducible transcripts were focused to extract for further analysis.

Real-Time Polymerase Chain Reaction

Three high-calcified plaques (H4: 797.6, H5: 995.5, H6: 2244.2) and 3 low-calcified plaques (L4: 2.0, L5: 4.8, L6: 95.0) were used for real-time polymerase chain reaction (PCR) analysis for angiogenesis or growth factor–related transcripts expressed differently by microarray analysis. Five hundred nanograms of total RNA from each sample was reverse transcribed with oligodT and random hexamer primers using Transcriptor First Strand cDNA Synthesis Kit (Roche Diagnostics, Basel, Switzerland). Twenty microliters reactions containing 3 μL cDNA and gene-specific primers were added to SYBRGreen I Master

Table 1. *Characteristics of the plaques and the clinical data*

Plaque	Ca score	Hemorrhage	Ulcer	Age	Gender	Stenosis (%)	Symptom	Hypertension	Diabetes	Dyslipidemia	Smoking	Antiplatelet	Anticoagulant	Renal malfunction
H1	558.4	+	−	73	M	83.0	A	+	+	+	+	+	−	−
H2	323.7	−	−	63	M	90.0	S	+	−	+	+	+	−	−
H3	434.0	−	−	70	M	85.0	A	+	−	−	+	+	−	−
H4	797.6	+	−	70	M	80.0	S	+	−	+	+	+	−	−
H5	995.5	−	−	65	M	95.0	S	+	−	+	+	+	−	−
H6	2244.2	−	−	70	M	76.5	S	−	−	+	+	+	−	−
H7	911.1	−	−	74	F	60.0	S	+	−	−	−	+	−	−
H8	680.9	−	−	66	F	90.0	S	+	−	+	+	+	−	−
H9	614.0	−	−	63	M	95.0	S	−	+	−	+	+	−	−
L1	38.8	+	−	67	M	80.0	S	+	+	+	−	+	−	−
L2	68.3	−	−	67	M	78.0	A	−	−	−	−	+	−	−
L3	98.0	+	+	74	F	90.0	S	+	−	−	+	+	−	−
L4	2.0	+	+	73	M	81.5	S	−	−	+	+	+	−	−
L5	4.8	+	+	66	M	73.0	S	+	+	+	+	+	−	−
L6	95.0	−	−	76	M	90.0	S	+	−	−	+	+	−	−
L7	26.6	+	−	68	M	75.0	S	−	−	+	−	+	−	−
L8	55.5	+	+	60	M	83.0	A	−	+	+	+	+	−	−
L9	83.5	−	−	74	M	75.0	S	+	−	−	+	+	+	−

Abbreviations: A, asymptomatic; F, female; M, male; H1-H9, high-calcified plaques; L1-L9, low-calcified plaques; S, symptomatic.

Table 2. *All angiogenesis and growth factor–related transcripts detected in microarray analysis for high- and low-calcified carotid plaques*

No.	Probe set ID	Probe ID	Representative public ID	Gene symbol	Gene title	Average log2 ratio
1	213176_s_at	HU133p2_22479	AI910869	LTBP4	Latent transforming growth factor beta binding protein 4	1.73
2	204200_s_at	HU133p2_13648	NM_002608	PDGFB	Platelet-derived growth factor beta polypeptide (simian sarcoma viral (v-sis) oncogene homolog)	1.24
3	201508_at	HU133p2_10957	NM_001552	IGFBP4	Insulin-like growth factor–binding protein 4	1.22
4	223333_s_at	HU133p2_32611	AF169312	ANGPTL4*	Angiopoietin-like protein 4	1.17
5	231762_at	HU133p2_41017	NM_004465	FGF10	Fibroblast growth factor 10	1.12
6	207334_s_at	HU133p2_16779	NM_003242	TGFBR2	Transforming growth factor, beta receptor II (70/80 kDa)	1.08
7	220789_s_at	HU133p2_30074	NM_004749	TBRG4	Transforming growth factor beta regulator 4	1.08
8	223836_at	HU133p2_33113	AB021123	FGFBP2	Fibroblast growth factor–binding protein 2	1.04
9	207822_at	HU133p2_17262	NM_023107	FGFR1	Fibroblast growth factor receptor 1	1.04
10	1555997_s_at	HU133p2_02723	BM128432	IGFBP5	Insulin-like growth factor–binding protein 5	.97
11	209908_s_at	HU133p2_19315	BF061658	TGFB2	Transforming growth factor, beta 2	.93
12	203425_s_at	HU133p2_12873	NM_000599	IGFBP5	Insulin-like growth factor–binding protein 5	.92
13	216061_x_at	HU133p2_25354	AU150748	PDGFB	Platelet-derived growth factor beta polypeptide (simian sarcoma viral (v-sis) oncogene homolog)	.90
14	221009_s_at	HU133p2_30294	NM_016109	ANGPTL4	Angiopoietin-like protein 4	.90
15	204442_x_at	HU133p2_13890	NM_003573	LTBP4	Latent transforming growth factor beta binding protein 4	.81
16	203424_s_at	HU133p2_12872	AW157548	IGFBP5	Insulin-like growth factor–binding protein 5	.76
17	211513_s_at	HU133p2_20840	AF172449	OGFR	Opioid growth factor receptor	.71
18	210973_s_at	HU133p2_20341	M63889	FGFR1	Fibroblast growth factor receptor 1	.70
19	227760_at	HU133p2_37015	AL522781	IGFBPL1	Insulin-like growth factor–binding protein-like 1	.69
20	223321_s_at	HU133p2_32599	AF312678	FGFRL1	Fibroblast growth factor receptor-like 1	.69
21	1561365_at	HU133p2_05958	AA609131	NRP1	Vascular endothelial cell growth factor 165 receptor/neuropilin (VEGF165)	.67
22	1552721_a_at	HU133p2_00329	NM_033136	FGF1	Fibroblast growth factor 1 (acidic)	.67
23	1552939_at	HU133p2_00488	NM_139290	ANGPT1	Angiopoietin 1	.67
24	210628_x_at	HU133p2_20014	AF051344	LTBP4	Latent transforming growth factor beta binding protein 4	.65
25	209542_x_at	HU133p2_18956	M29644	IGF1	Insulin-like growth factor 1 (somatomedin C)	.64
26	210998_s_at	HU133p2_20366	M77227	HGF	Hepatocyte growth factor (hepapoietin A; scatter factor)	.64
27	219922_s_at	HU133p2_29207	NM_021070	LTBP3	Latent transforming growth factor beta binding protein 3	.63
28	243799_x_at	HU133p2_53050	T40942	ANGPTL3	Angiopoietin-like 3, mRNA (cDNA clone IMAGE:3934961)	.61
29	202718_at	HU133p2_12167	NM_000597	IGFBP2	Insulin-like growth factor–binding protein 2, 36 kDa	.61
30	203683_s_at	HU133p2_13131	NM_003377	VEGFB	Vascular endothelial growth factor B	.60
31	205117_at	HU133p2_14565	X59065	FGF1	Fibroblast growth factor 1 (acidic)	.60
32	220961_s_at	HU133p2_30246	NM_030900	TBRG4	Transforming growth factor beta regulator 4	.59
33	201506_at	HU133p2_10955	NM_000358	TGFBI	Transforming growth factor, beta-induced, 68 kDa	.58
34	211958_at	HU133p2_21266	R73554	IGFBP5	Insulin-like growth factor–binding protein 5	.56
35	202273_at	HU133p2_11722	NM_002609	PDGFRB	Platelet-derived growth factor receptor, beta polypeptide	.56
36	204731_at	HU133p2_14179	NM_003243	TGFBR3	Transforming growth factor, beta receptor III	.56

37	205608_s_at	HU133p2_15056	U83508	ANGPT1	Angiopoietin 1	.55
38	237261_at	HU133p2_46511	BE501356	ANGPT2	Angiopoietin 2	.55
39	213910_at	HU133p2_23210	AW770896	IGFBP7	Insulin-like growth factor–binding protein 7	.54
40	210443_x_at	HU133p2_19842	AF172452	OGFR	Opioid growth factor receptor	.54
41	201984_s_at	HU133p2_11433	NM_005228	EGFR	Epidermal growth factor receptor (erythroblastic leukemia viral (v-erb-b) oncogene homolog, avian)	.53
42	206814_at	HU133p2_16261	NM_002506	NGF	Nerve growth factor (beta polypeptide)	.52
43	235277_at	HU133p2_44527	BG334930	AMOTL1	Angiomotin-like 1	.52
44	203085_s_at	HU133p2_12535	BC000125	TGFB1	Transforming growth factor, beta 1	.51
45	226625_at	HU133p2_35881	AW193698	TGFBR3	Transforming growth factor, beta receptor III	.51
46	203851_at	HU133p2_13299	NM_002178	IGFBP6	Insulin-like growth factor–binding protein 6	.51
47	242701_at	HU133p2_51951	AW977978	TBRG1	Transforming growth factor beta regulator 1	.50
48	201983_s_at	HU133p2_11432	AW157070	EGFR	Epidermal growth factor receptor (erythroblastic leukemia viral (v-erb-b) oncogene homolog, avian)	.50
49	207501_s_at	HU133p2_16944	NM_004113	FGF12	Fibroblast growth factor 12	.48
50	209540_at	HU133p2_18954	AU144912	IGF1	Insulin-like growth factor 1 (somatomedin C)	.47
51	212143_s_at	HU133p2_21450	BF340228	IGFBP3	Insulin-like growth factor–binding protein 3	.47
52	205210_at	HU133p2_14658	NM_004257	TGFBRAP1	Transforming growth factor, beta receptor associated protein 1	.46
53	1557285_at	HU133p2_03547	AI891075	AREGB	PREDICTED: *Homo sapiens* similar to amphiregulin precursor, mRNA	.46
54	231382_at	HU133p2_40637	AI798863	FGF18	Fibroblast growth factor 18, mRNA (cDNA clone MGC: 10529 IMAGE: 3948893)	.45
55	211599_x_at	HU133p2_20925	U19348	MET	Met proto-oncogene (hepatocyte growth factor receptor)	.44
56	210764_s_at	HU133p2_20146	AF003114	CYR61	Cysteine-rich, angiogenic inducer, 61	.43
57	211527_x_at	HU133p2_20854	M27281	VEGFA	Vascular endothelial growth factor A	.43
58	211148_s_at	HU133p2_20512	AF187858	ANGPT2	Angiopoietin 2	.42
59	205016_at	HU133p2_14464	NM_003236	TGFA	Transforming growth factor, alpha	.42
60	238469_at	HU133p2_47719	BE620374	OGFRL1	Opioid growth factor receptor-like 1	.42
61	209541_at	HU133p2_18955	AI972496	IGF1	Insulin-like growth factor 1 (somatomedin C)	.42
62	213004_at	HU133p2_22308	AI074333	ANGPTL2	Angiopoietin-like 2	.41
63	205463_s_at	HU133p2_14911	NM_002607	PDGFA	Platelet-derived growth factor alpha polypeptide	.41
64	222860_s_at	HU133p2_32140	AB033832	PDGFD	Platelet-derived growth factor D	.41
65	213001_at	HU133p2_22305	AF007150	ANGPTL2	Angiopoietin-like 2	.41
66	203426_s_at	HU133p2_12874	M65062	IGFBP5	Insulin-like growth factor–binding protein 5	.41
67	209652_s_at	HU133p2_19062	BC001422	PGF	Placental growth factor	.40
68	209410_s_at	HU133p2_18824	AF000017	GRB10	Growth factor receptor-bound protein 10	.39
69	206589_at	HU133p2_16036	NM_005263	GFI1	Growth factor independent 1 transcription repressor	.36
70	211577_s_at	HU133p2_20903	M37484	IGF1	Insulin-like growth factor 1 (somatomedin C)	.35
71	219514_at	HU133p2_28799	NM_012098	ANGPTL2	Angiopoietin-like 2	.35
72	204659_s_at	HU133p2_14107	AF124604	GFER	Growth factor, augmenter of liver regeneration	.35
73	201289_at	HU133p2_10738	NM_001554	CYR61	Cysteine-rich, angiogenic inducer, 61	.35
74	202841_x_at	HU133p2_12291	NM_007346	OGFR	Opioid growth factor receptor	.34
75	203627_at	HU133p2_13075	AI830698	IGF1R	Insulin-like growth factor 1 receptor	.33

(*Continued*)

Table 2. (*Continued*)

No.	Probe set ID	Probe ID	Representative public ID	Gene symbol	Gene title	Average log2 ratio
76	203002_at	HU133p2_12452	NM_016201	AMOTL2	Angiomotin-like 2	.33
77	222719_s_at	HU133p2_31999	AB033831	PDGFC	Platelet-derived growth factor C	.32
78	209747_at	HU133p2_19156	J03241	TGFB3	Transforming growth factor, beta 3	.31
79	210755_at	HU133p2_20137	U46010	HGF	Hepatocyte growth factor (hepapoietin A; scatter factor)	.30
80	205638_at	HU133p2_15086	NM_001704	BAI3	Brain-specific angiogenesis inhibitor 3	.30
81	209409_at	HU133p2_18823	D86962	GRB10	Growth factor receptor-bound protein 10	.29
82	206254_at	HU133p2_15701	NM_001963	EGF	Epidermal growth factor (beta-urogastrone)	.27
83	211535_s_at	HU133p2_20862	M60485	FGFR1	Fibroblast growth factor receptor 1	.27
84	211959_at	HU133p2_21267	AW007532	IGFBP5	Insulin-like growth factor–binding protein 5	.26
85	221976_s_at	HU133p2_31257	AW207448	HDGFRP3	Hepatoma-derived growth factor 2 (HDGF2)	.25
86	209651_at	HU133p2_19061	BC001830	TGFB1I1	Transforming growth factor beta 1–induced transcript 1	.25
87	208240_s_at	HU133p2_17665	NM_013394	FGF1	Fibroblast growth factor 1 (acidic)	.22
88	204682_at	HU133p2_14130	NM_000428	LTBP2	Latent transforming growth factor beta binding protein 2	.22
89	205572_at	HU133p2_15020	NM_001147	ANGPT2	Angiopoietin 2	.22
90	225330_at	HU133p2_34588	AL044092	IGF1R	Insulin-like growth factor 1 receptor	.21
91	228121_at	HU133p2_37376	AU145950	TGFB2	Transforming growth factor, beta 2	.21
92	209909_s_at	HU133p2_19316	M19154	TGFB2	Transforming growth factor, beta 2	.20
93	209101_at	HU133p2_18516	M92934	CTGF	Connective tissue growth factor	.19
94	215248_at	HU133p2_24543	AU145003	GRB10	Growth factor receptor-bound protein 10	.18
95	203084_at	HU133p2_12534	NM_000660	TGFB1	Transforming growth factor, beta 1	.18
96	224339_s_at	HU133p2_33607	AB056476	ANGPTL1	Angiopoietin-like 1	.16
97	209960_at	HU133p2_19367	X16323	HGF	Hepatocyte growth factor (hepapoietin A; scatter factor)	.16
98	1555103_s_at	HU133p2_02066	BC010956	FGF7	Fibroblast growth factor 7 (keratinocyte growth factor)	.16
99	208042_at	HU133p2_17472	NM_013303	AGGF1	Angiogenic factor with G patch and FHA domains 1	.15
100	230231_at	HU133p2_39486	BE549937	FGF14	Fibroblast growth factor 14	.14
101	228266_s_at	HU133p2_37521	BE703418	HDGFRP3	Hepatoma-derived growth factor, related protein 3	.14
102	210513_s_at	HU133p2_19904	AF091352	VEGFA	Vascular endothelial growth factor A	.13
103	223690_at	HU133p2_32967	AF113211	LTBP2	Latent transforming growth factor beta binding protein 2	.13
104	227308_x_at	HU133p2_36564	AW515704	LTBP3	Latent transforming growth factor beta binding protein 3	.12
105	220407_s_at	HU133p2_29692	NM_003238	TGFB2	Transforming growth factor, beta 2	.12
106	204422_s_at	HU133p2_13870	NM_002006	FGF2	Fibroblast growth factor 2 (basic)	.12
107	222112_at	HU133p2_31393	AV710549	EPS15L1	Epidermal growth factor receptor pathway substrate 15-like 1	.10
108	230681_at	HU133p2_39936	AI279879	TBRG1	Transforming growth factor beta regulator 1	.10
109	236034_at	HU133p2_45284	AA083514	ANGPT2	Angiopoietin 2	.10
110	209961_s_at	HU133p2_19368	M60718	HGF	Hepatocyte growth factor (hepapoietin A; scatter factor)	.10
111	203628_at	HU133p2_13076	H05812	IGF1R	Insulin-like growth factor 1 receptor	.10
112	205609_at	HU133p2_15057	NM_001146	ANGPT1	Angiopoietin 1	.07
113	215075_s_at	HU133p2_24370	L29511	GRB2	Growth factor receptor-bound protein 2	.07
114	205226_at	HU133p2_14674	NM_006207	PDGFRL	Platelet-derived growth factor receptor-like	.06

115	209526_s_at	HU133p2_18940	AB029156	HDGFRP3	Hepatoma-derived growth factor, related protein 3	.06
116	206987_x_at	HU133p2_16434	NM_003862	FGF18	Fibroblast growth factor18	.06
117	210999_s_at	HU133p2_20367	U66065	GRB10	Growth factor receptor-bound protein 10	.05
118	238453_at	HU133p2_47703	AI628573	FGFBP3	Fibroblast growth factor–binding protein 3	.04
119	201392_s_at	HU133p2_10841	BG031974	IGF2R	Insulin-like growth factor 2 receptor	.03
120	216867_s_at	HU133p2_26158	X03795	PDGFA	Platelet-derived growth factor alpha polypeptide	.02
121	215404_x_at	HU133p2_24699	AK024388	FGFR1	Fibroblast growth factor receptor 1	.02
122	225450_at	HU133p2_34708	AI433831	AMOTL1	Angiomotin-like 1	.01
123	202728_s_at	HU133p2_12177	AI986120	LTBP1	Latent transforming growth factor beta binding protein 1	.00
124	203821_at	HU133p2_13269	NM_001945	HBEGF	Heparin-binding EGF-like growth factor	.00
125	205110_s_at	HU133p2_14558	NM_004114	FGF13	Fibroblast growth factor 13	−.01
126	223049_at	HU133p2_32329	AF246238	GRB2	Growth factor receptor-bound protein 2	−.01
127	202409_at	HU133p2_11858	X07868	IGF2///INS-IGF2	Insulin-like growth factor 2 (somatomedin A)///INS-IGF2 readthrough transcript	−.03
128	231773_at	HU133p2_41028	BF002046	ANGPTL1	Angiopoietin-like 1	−.03
129	210428_s_at	HU133p2_19827	AF260566	HGS	Hepatocyte growth factor–regulated tyrosine kinase substrate	−.05
130	226705_at	HU133p2_35961	BE467261	FGFR1	Fibroblast growth factor receptor 1	−.05
131	203131_at	HU133p2_12580	NM_006206	PDGFRA	Platelet-derived growth factor receptor, alpha polypeptide	−.05
132	222164_at	HU133p2_31445	AU145411	FGFR1	Fibroblast growth factor receptor 1	−.07
133	219304_s_at	HU133p2_28589	NM_025208	PDGFD	Platelet-derived growth factor D	−.07
134	202729_s_at	HU133p2_12178	NM_000627	LTBP1	Latent transforming growth factor beta binding protein 1	−.07
135	216693_x_at	HU133p2_25984	AL133102	HDGFRP3	Hepatoma-derived growth factor, related protein 3	−.07
136	207937_x_at	HU133p2_17374	NM_023110	FGFR1	Fibroblast growth factor receptor 1	−.08
137	205302_at	HU133p2_14750	NM_000596	IGFBP1	Insulin-like growth factor–binding protein 1	−.09
138	38037_at	HU133p2_54303	M60278	HBEGF	Heparin-binding EGF-like growth factor	−.09
139	210512_s_at	HU133p2_19903	AF022375	VEGFA	Vascular endothelial growth factor A	−.09
140	225459_at	HU133p2_34717	AU157155	AMOTL1	Angiomotin-like 1	−.13
141	209524_at	HU133p2_18938	AK001280	HDGFRP3	Hepatoma-derived growth factor, related protein 3	−.13
142	218847_at	HU133p2_28132	NM_006548	IGF2BP2	Insulin-like growth factor 2 mRNA-binding protein 2	−.15
143	201494_at	HU133p2_10943	NM_005040	PRCP	Prolylcarboxypeptidase (angiotensinase C)	−.17
144	202609_at	HU133p2_12058	NM_004447	EPS8	Epidermal growth factor receptor pathway substrate 8	−.19
145	203820_s_at	HU133p2_13268	NM_006547	IGF2BP3	Insulin-like growth factor 2 mRNA-binding protein 3	−.22
146	212171_x_at	HU133p2_21478	H95344	VEGFA	Vascular endothelial growth factor A	−.23
147	201393_s_at	HU133p2_10842	NM_000876	IGF2R	Insulin-like growth factor 2 receptor	−.23
148	218718_at	HU133p2_28003	NM_016205	PDGFC	Platelet-derived growth factor C	−.25
149	211485_s_at	HU133p2_20813	AF211188	FGF18	Fibroblast growth factor 18	−.28
150	211568_at	HU133p2_20894	AB011122	BAI3	Brain-specific angiogenesis inhibitor 3	−.29
151	232680_at	HU133p2_41935	AI352424	HDGFL1	Hepatoma-derived growth factor-like 1	−.31
152	239183_at	HU133p2_48433	W67461	ANGPTL1	Angiopoietin-like 1	−.31
153	204379_s_at	HU133p2_13827	NM_000142	FGFR3	Fibroblast growth factor receptor 3	−.33
154	208441_at	HU133p2_17861	NM_015883	IGF1R	Insulin-like growth factor 1 receptor	−.33

(*Continued*)

Table 2. (*Continued*)

No.	Probe set ID	Probe ID	Representative public ID	Gene symbol	Gene title	Average log2 ratio
155	231031_at	HU133p2_40286	AI761573	KGFLP2	Keratinocyte growth factor–like protein 2	−.34
156	208228_s_at	HU133p2_17654	M87771	FGFR2	Fibroblast growth factor receptor 2	−.36
157	211029_x_at	HU133p2_20396	BC006245	FGF18	Fibroblast growth factor 18	−.38
158	209521_s_at	HU133p2_18935	AF286598	AMOT	Angiomotin	−.39
159	228699_at	HU133p2_37954	AI741712	NRP2	Vascular endothelial cell growth factor 165 receptor 2 (VEGF165R2)	−.40
160	211551_at	HU133p2_20877	K03193	EGFR	Epidermal growth factor receptor (erythroblastic leukemia viral (v-erb-b) oncogene homolog, avian)	−.42
161	204421_s_at	HU133p2_13869	M27968	FGF2	Fibroblast growth factor 2 (basic)	−.42
162	205782_at	HU133p2_15230	NM_002009	FGF7	Fibroblast growth factor 7 (keratinocyte growth factor)	−.44
163	205586_x_at	HU133p2_15034	NM_003378	VGF	VGF nerve growth factor inducible	−.44
164	203819_s_at	HU133p2_13267	AU160004	IGF2BP3	Insulin-like growth factor 2 mRNA-binding protein 3	−.47
165	215305_at	HU133p2_24600	H79306	PDGFRA	Platelet-derived growth factor receptor, alpha polypeptide	−.49
166	1554741_s_at	HU133p2_01794	AF523265	FGF7///KGFLP1///KGFLP2	Fibroblast growth factor 7 (keratinocyte growth factor)///keratinocyte growth factor–like protein 1	−.57
167	230288_at	HU133p2_39543	AW418619	FGF14	Fibroblast growth factor 14	−.64
168	209946_at	HU133p2_19353	U58111	VEGFC	Vascular endothelial growth factor C	−.82
169	230410_at	HU133p2_39665	N25995	NRP2	Vascular endothelial cell growth factor 165 receptor 2 (VEGF165R2)	−.91
170	206204_at	HU133p2_15651	NM_004490	GRB14	Growth factor receptor-bound protein 14	−.96
171	219803_at	HU133p2_29088	NM_014495	ANGPTL3	Angiopoietin-like 3	−1.10
172	231684_at	HU133p2_40939	AV659209	ANGPTL3	Angiopoietin-like 3, mRNA (cDNA clone IMAGE: 3934961)	−1.47
173	203638_s_at	HU133p2_13086	NM_022969	FGFR2†	Fibroblast growth factor receptor 2	−1.84
174	207750_at	HU133p2_17192	NM_018510	EPS15L2	Epidermal growth factor receptor pathway substrate 15-like 2	−2.22
175	206423_at	HU133p2_15870	NM_021146	ANGPTL7	Angiopoietin-like 7	−2.40

Abbreviations: cDNA, complementary DNA; mRNA, messenger RNA.
*More than 5 of comparison sets showing (log2 ratio ≥ 1 and the detection call of the highly calcified plaque "P").
†More than 5 of comparison sets showing (log2 ratio ≤ −1 and the detection call of the low-calcified plaque "P").

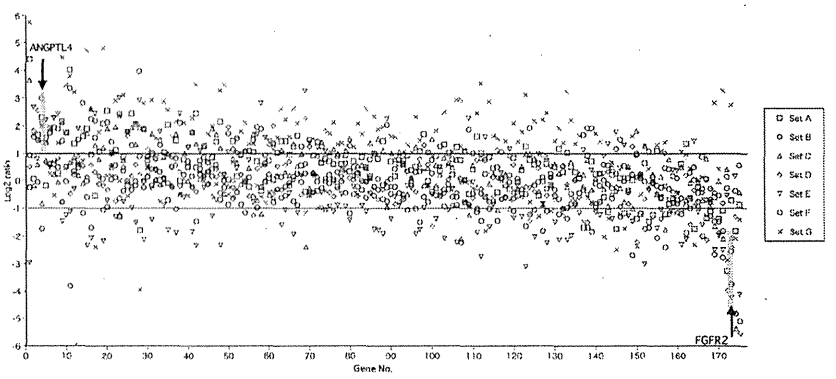

Figure 1. *Results of microarray analysis. GeneChip analysis showed 93 angiogenesis or growth factor–related transcripts reliably expressed (175 probe sets). Among them, ANGPTL4 and FGFR2 genes showed significant difference to fulfill the following criteria: (1) (log2 ratio ≥ 1 and the detection call of the highly calcified plaque "P [present]") in more than 5 of 7 comparison sets or (2) (log2 ratio ≤ −1 and the detection call of the low-calcified plaque "P") in more than 5 of 7 comparison sets. Gene numbers correspond to those shown in Table 2 in the order of average log2 ratio. Abbreviations: ANGPTL4, angiopoietin-like protein 4; FGFR2, fibroblast growth factor receptor 2.*

(Roche Diagnostics) mix solution and were run in duplicate in a LightCycler480 (Roche Diagnostics) (1 cycle at 95°C for 10 min, 40 cycles at 95°C for 10 s, 60°C for 10 s, and 72°C for 10 s (target genes) or 20 s (β-actin). The amplified transcripts were quantified by comparative computed tomography method using human β-actin as the internal control. The primer sequences on the basis of GenBank accession numbers were as follows: human angiopoietin-like protein 4 (ANGPTL4; NM_139314.1, 124 bp)—forward: 5′-ACT TGG GAC CAG GAT CAC GA-3′ and reverse: 5′-GTG GGA TGG AGV GGA AGT-3′; human fibroblast growth factor receptor 2 (FGFR2; NM_000141.4, 98 bp)—forward: 5′-AAC GGG AAG GAG TTT AAG CA-3′ and reverse 5′-TTG TCA GAT GGG ACC ACA CT-3′.

Western Blotting

Three high-calcified plaques (H7: 911.1, H8: 680.9, H9: 614.0) and 3 low-calcified plaques (L7: 26.6, L8: 55.5, L9: 83.5) were used for Western blotting analysis. Total cellular proteins were isolated with T-PER tissue protein extraction reagent (Thermo Scientific, Pierce Biotechnology, Rockford, IL). Proteins were quantitated by BCA protein assay reagent (Pierce Biotechnology), and equal amounts of protein from each sample (10 μg per lane) were separated on 10% sodium dodecyl sulfate–polyacrylamide gel electrophoresis followed by electroblotting to polyvinylidene difluoride membranes (Hybond P; GE Healthcare, Buckinghamshire, UK). Membranes were blocked in 1% skimmed milk and .1% Tween 20 in phosphate-buffered saline. ANGPTL4 was detected using mouse polyclonal antibody (1:500; Abnova, Taipei, Taiwan). FGFR2 was detected using mouse monoclonal antibodies (1:200; Abnova). The secondary antibody was horseradish peroxidase–conjugated rabbit anti-mouse immunoglobulin (IgG; 1:400,000; Millipore, Merck Millipore, Billerica, MA). Proteins were visualized using ECL Plus Western Blotting Detection Reagents (GE Healthcare). Semiquantitative analysis of protein concentration from Western blots was performed using a scanner with analyzing software (Scion Image; Scion Co., Frederick, MD).

Immunohistochemistry

The same plaques used in Western blotting analysis were also applied for immunohistochemistry. Paraformaldehyde-fixed sections of the specimens were embedded in paraffin. The sections were deparaffinized, rinsed in Tris-buffered saline (TBS), and treated with .3% hydrogen peroxide in methanol (30 min at room temperature). Slides were placed in DAKO Protein Block (Dako, Glostrup, Denmark) for 10 minutes before Avidin/Biotin Blocking Kit (SP-2001; Vector Laboratories, Burlingame, CA) was applied. Primary antibodies (ANGPTL4 mouse monoclonal antibody, 1:500, ALX-804-723; ENZO Life Sciences, Farmingdale, NY; FGFR2 mouse monoclonal antibody, 1:500, Abnova H00002263-M01) were added, and sections were incubated overnight at 4°C. Anti-rabbit Biotin (E0432; Dako) was applied following rinsing in TBS, and the slides were incubated for 30 minutes at room temperature. The streptavidin–peroxidase complex (426062; Nichirei, Tokyo, Japan) was then used, and the sections were incubated for 5 minutes followed by rinsing in TBS. Diaminobenzidine was used as the chromogen and counterstained with hematoxylin. Mouse IgG1 (X0931; Dako) and Mouse IgG2b (MAB0042; R&D Systems, Minneapolis, MN) served as negative controls, respectively.

Statistical Analysis

All statistical evaluations were performed with statistical software (Statview version 5.0; SPS, NC), and all results are presented as mean ± SEM values. The Mann–Whitney *U* test was used to compare the expression of real-time PCR and the signal intensities of Western blotting analysis for high- and low-calcified plaques and to compare the degrees of stenosis between them. Values of *P* less than .01 were considered significant.

Table 3. *Representative calcification/osteogenesis-related transcripts detected in microarray analysis for high- and low-calcified carotid plaques*

No.	Probe set ID	Probe ID	Representative public ID	Gene symbol	Gene title	Average log2 ratio
1	1559201_a_at	HU133p2_04651	BU929456	OSTF1	Osteoclast stimulating factor	.63
2	204114_at	HU133p2_13562	NM_007361	NID2	Nidogen 2 (osteonidogen)	.62
3	218730_s_at	HU133p2_28015	NM_014057	OGN	Osteoglycin	.53
4	222722_at	HU133p2_32002	AV700059	OGN	Osteoglycin	.29
5	204479_at	HU133p2_13927	NM_012383	OSTF1	Osteoclast stimulating factor 1	.27
6	204832_s_at	HU133p2_14280	NM_004329	BMPR1A	Bone morphogenetic protein receptor, type IA	.16
7	236179_at	HU133p2_45429	AI754693	CDH11	Cadherin 11, type 2, OB-cadherin (osteoblast)	.16
8	225144_at	HU133p2_34402	AI457436	BMPR2	Bone morphogenetic protein receptor, type II (serine/ threonine kinase)	.14
9	206176_at	HU133p2_15623	NM_001718	BMP6	Bone morphogenetic protein 6	.13
10	221615_at	HU133p2_30898	AF104013	BMP8A/// BMP8B	Bone morphogenetic protein 8a///bone morphogenetic protein 8b	.07
11	231873_at	HU133p2_41128	AL046696	BMPR2	Bone morphogenetic protein receptor, type II (serine/ threonine kinase)	.07
12	205908_s_at	HU133p2_15356	NM_005014	OMD	Osteomodulin	.06
13	213578_at	HU133p2_22879	AI678679	BMPR1A	Bone morphogenetic protein receptor, type IA	.06
14	207172_s_at	HU133p2_16618	NM_001797	CDH11	Cadherin 11, type 2, OB-cadherin (osteoblast)	.04
15	205289_at	HU133p2_14737	AA583044	BMP2	Bone morphogenetic protein 2	.03
16	238516_at	HU133p2_47766	BF247383	BMPR2	Bone morphogenetic protein receptor, type II (serine/ threonine kinase)	−.04
17	1554503_a_at	HU133p2_01617	BC035023	OSCAR	Osteoclast associated, immunoglobulin-like receptor	−.05
18	207173_x_at	HU133p2_16619	D21254	CDH11	Cadherin 11, type 2, OB-cadherin (osteoblast)	−.08
19	212667_at	HU133p2_21973	AL575922	SPARC	Secreted protein, acidic, cysteine rich (osteonectin)	−.09
20	239286_at	HU133p2_48536	AI038737	CDH11	Cadherin 11, type 2, OB-cadherin (osteoblast)	−.10
21	205290_s_at	HU133p2_14738	NM_001200	BMP2	Bone morphogenetic protein 2	−.13
22	243287_s_at	HU133p2_52538	H04482	OSTM1	Osteopetrosis-associated transmembrane protein 1	−.13
23	205907_s_at	HU133p2_15355	AI765819	OMD	Osteomodulin	−.19
24	231993_at	HU133p2_41248	AK026784	ITGBL1	Osteoblast-specific cysteine-rich protein	−.21
25	1555778_a_at	HU133p2_02565	AY140646	POSTN	Periostin, osteoblast-specific factor	−.28
26	202363_at	HU133p2_11812	AF231124	SPOCK1	Sparc/osteonectin, cwcv, and kazal-like domains proteoglycan (testican) 1	−.34
27	241141_at	HU133p2_50391	AI968068	BMP6	CDNA FLJ51307 complete cds, highly similar to bone morphogenetic protein 6 precursor	−.54

(Continued)

Table 3. (*Continued*)

No.	Probe set ID	Probe ID	Representative public ID	Gene symbol	Gene title	Average log2 ratio
28	1557079_at	HU133p2_03426	AI753143	ITGBL1	Osteoblast-specific cysteine-rich protein	−.71
29	229975_at	HU133p2_39230	AI826437	BMPR1B	Bone morphogenetic protein receptor, type IB	−.77
30	242579_at	HU133p2_51829	AA935461	BMPR1B	Bone morphogenetic protein receptor, type IB	−1.00
31	206434_at	HU133p2_15881	NM_016950	SPOCK3	Sparc/osteonectin, cwcv, and kazal-like domains proteoglycan (testican) 3	−1.61

Results

Microarray

GeneChip analysis showed 93 angiogenesis or growth factor–related transcripts reliably expressed (175 probe sets, Table 2 and Fig 1). Among them, 2 genes showed significant difference to fulfill the criteria: (1) (log2 ratio ≥ 1 and the detection call of the highly calcified plaque "P") in more than 5 of 7 comparison sets or (2) (log2 ratio ≤ −1 and the detection call of the low-calcified plaque "P") in more than 5 of 7 comparison sets. ANGPTL4 expression was significantly elevated, whereas FGFR2 expression was significantly suppressed in the high-calcified plaques.

As for calcification or osteogenesis-related factors and hypoxia-inducible factors, 19 transcripts in 31 probe sets (Table 3 and Fig 2) and 3 transcripts in 6 probe sets (Table 4 and Fig 3) expressed, respectively, but no genes showed significant difference to fulfill the above criteria.

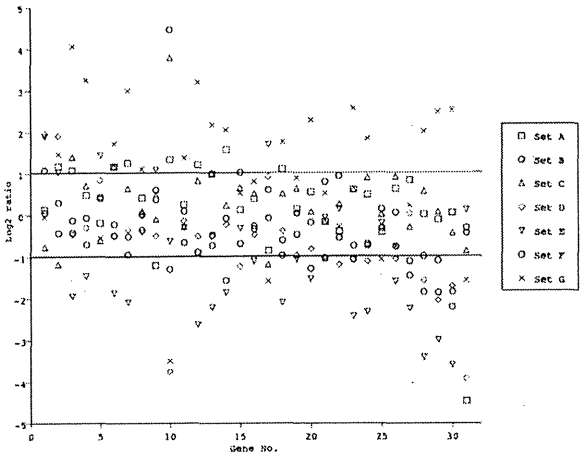

Figure 2. *Results of microarray analysis. As for calcification or osteogenesis-related factors and hypoxia-inducible factors, 19 transcripts in 31 probe sets expressed, but no genes showed significant difference to fulfill the present criteria. Gene numbers correspond to those shown in Table 3 in the order of average log2 ratio.*

Significant expression of osteopontin (BSP-1, BNSP, ETA-1, and SPP1) was not observed in our series.

Real-Time PCR

ANGPTL4 and FGFR2 were analyzed by quantitative real-time PCR. The messenger RNA (mRNA) expression of ANGPTL4 was significantly higher in highly calcified plaques, and mRNA expression of FGFR2 was lower than low-calcified plaques, revealing 1.28-fold induction for ANGPTL4 and .58-fold induction for FGFR2 (both $P < .001$) (Fig 4).

Western Blotting

Western blotting was used to quantify the relative protein expression of ANGPTL4 and FGFR2 for high- and low-calcified plaques. The expression of ANGPTL4 protein with high-calcified plaques was significantly higher than that of one with low-calcified plaques, whereas FGFR2 protein expression was significantly lower ($P < .001$, respectively, Fig 5, A,B).

Immunohistochemistry

Immunohistochemistry showed increased expression of ANGPTL4 in endothelial cells and in smooth muscle cells of the intima of high-calcified plaques (Fig 6, C). FGFR2 staining was not remarkable in high-calcified plaques, whereas strong immunoreactivity was observed mainly in the intimal smooth muscle cells of low-calcified plaques (Fig 6, G).

Discussion

In the present study, we first demonstrated increased gene and protein expression of ANGPTL4 in high-calcified plaques, whereas the expression of FGFR2 was suppressed and was rather remarkable in low-calcified plaques.

Most of the investigators who have studied gene expression in carotid plaques have focused on the difference

Table 4. *Hypoxia-inducible factors/protein-related transcripts detected in microarray analysis for high- and low-calcified carotid plaques*

No.	Probe set ID	Probe ID	Representative public ID	Gene symbol	Gene title	Average log2 ratio
1	222124_at	HU133p2_31405	NM_173503	EFCAB3///LOC 100133744	EF hand calcium-binding domain 3///similar to hypoxia-inducible protein 2	1.72
2	218507_at	HU133p2_27793	AK021881	HIF3A	Hypoxia-inducible factor 3, alpha subunit	.46
3	1553392_at	HU133p2_00818	BC001863	HIG2	Hypoxia-inducible protein 2	.15
4	1556069_s_at	HU133p2_02771	NM_013332	HIG2	Hypoxia-inducible protein 2	−.26
5	1555318_at	HU133p2_02232	AK021881	HIF3A	Hypoxia inducible factor 3, alpha subunit	−.42
6	1554452_a_at	HU133p2_01578	BC026308	HIF3A	Hypoxia inducible factor 3, alpha subunit	−.63

between symptomatic and asymptomatic plaques. Vemuganti et al performed microarray analysis and revealed that the transcripts expressed more abundantly in the symptomatic plaques were those concerning active cell proliferation, neoplastic process, control ionic homeostasis, the progression of degenerative neurological diseases, and angiogenesis.[7,8] Razuvaev et al[9] disclosed that genes associated with inflammation (such as RANKL and CD68) were overexpressed in symptomatic compared with asymptomatic plaques using a database of clinical information and microarray data from 106 CEA. Wahlgren et al[10] confirmed the lower expression of proinflammatory factors (mRNA and protein expression for monocyte chemotactic protein-1 and interleukin-8) in calcified plaques compared with noncalcified plaques by real-time PCR and Western blotting. However, there has been no finding of more abundant gene expression detected by microarray analysis in highly calcified plaques compared with low-calcified plaques.

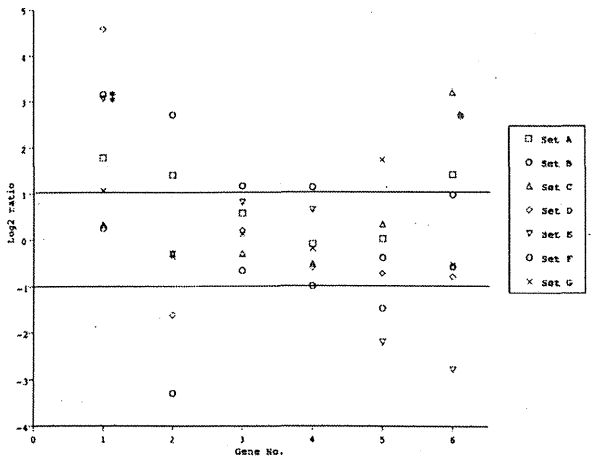

Figure 3. *Results of microarray analysis. As for hypoxia-inducible factors, 3 transcripts in 6 probe sets expressed, but no genes showed significant difference to fulfill the present criteria. "*," indicates the detection call of the highly calcified plaque "A (absent)." Gene numbers correspond to those shown in Table 4 in the order of average log2 ratio.*

ANGPTL4 is known as a hepatic fibrinogen/angiopoietin-related protein, fasting-induced adipose factor, peroxisome proliferator–activated receptors, and gamma angiopoietin–related protein. It is 1 of 7 members of the ANGPTL family (ANGPTL1-7).[11] ANGPTL4 was previously referred to as ANGPTL2 but has been renamed ANGPTL4. ANGPTL4 has been implicated in the regulation of angiogenesis and a variety of diseases including cardiovascular disease, wound repair, inflammation, and arthritis.

However, Ito et al[12] found that ANGPTL4 did not induce neovascularization in a corneal pocket assay. They showed that ANGPTL4 inhibits vascular endothelial growth factor (VEGF)–induced neovascularization. K14-ANGPTL4 transgenic mice show no evidence of increased vascularity in skin tissues compared with controls. Tumor angiogenesis was inhibited when tumors were transplanted into the skin of K14-ANGPTL4 mice, suggesting that ANGPTL4 is an antiangiogenic factor. Peroxisome proliferator–activated receptor γ is expressed in endothelial cells, and its ligands are potent negative modulators of angiogenesis.[13] ANGPTL4 is predicted to exert antiangiogenic effects.

On the other hand, the mammalian FGF family is composed of 18 ligands that elicit their actions through 4 highly conserved transmembrane tyrosine kinase receptors (FGFR1-4).[14] FGFs have functions such as cell proliferation, migration, differentiation, and angiogenesis in various cells and tissues. The angiogenic properties of FGF1 and 2 are well known. Specifically, FGF1 and 2 induce the promotion of endothelial cell proliferation and the physical organization of endothelial cells into tube-like structures.[15] Decreased expression of FGFR2 in the present study indicated that angiogenesis was suppressed in the heavily calcified plaques.

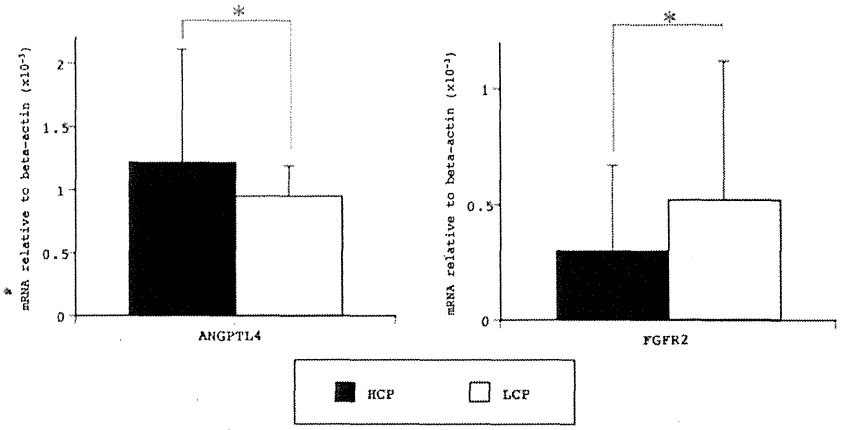

Figure 4. *Results of real-time polymerase chain reaction. The mRNA expression of ANGPTL4 was significantly higher in HCPs (H4-H6) and FGFR2 mRNA expression was lower than LCPs (L4-L6), revealing 1.28-fold induction for ANGPTL4 and .58-fold induction for FGFR2 (both P < .001). Abbreviations: ANGPTL4, angiopoietin-like protein 4; FGFR2, fibroblast growth factor receptor 2; HCP, high-calcified plaque; LCP, low-calcified plaque; mRNA, messenger RNA.*

Though Kadomatsu et al[16] reported that ANGPTL4 expression was induced by both chronic hypoxia and endoplasmic reticulum stress resulting from adipose tissue expansion, it is conceivable to think that ANGPTL4 was induced to perform an antiangiogenic modulating function rather than in response to the chronic hypoxia, considering the downregulation of FGFR2 in high-calcified plaques. This possibility is compatible with the result that other well-known hypoxia-inducible transcripts, HIF-1α and its family, which might lead to angiogenesis via expression of VEGF[17] were not upregulated nor VEGF. This is consistent with the fact that the highly calcified plaques contained fewer hemorrhages and ulcers compared with the low-calcified plaques as in our specimens. However, because the percentage of symptomatic cases was the same in high- and low-calcified plaque groups in the present study, the relationship between symptoms and ANGPTL4 expression was not apparent. However, many investigators have reported the association between hemorrhages or ulcers in carotid plaques and symptoms,[18-20] and there is a possibility that upregulation of ANGPTL4 may contribute to the stability of plaques at least in part. Because limited cases might affect the present result, further studies with larger numbers of patients may elucidate this point.

We could not observe any significant expression to fulfill the present criteria regarding calcification or osteogenesis-related genes in both groups. The expression of bone morphogenetic protein was reported to be increased at calcification site,[21] whereas transforming growth factor-β is produced by osteoblasts and released from the bone matrix and regulates bone metabolism. Osteoglycin interacts with transforming growth factor-β and induces bone formation.[22] The precise reason for no significant upregulation of these genes in high-calcified carotid plaques is not clear. There is a possibility of less association of these genes to formation of calcification in

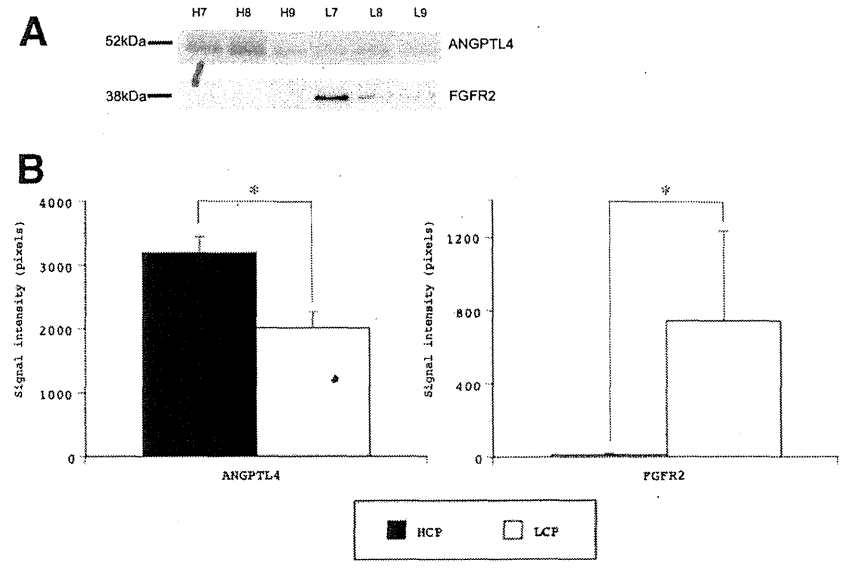

Figure 5. *Results of Western blotting analysis. Significantly more abundant expression of the ANGPTL4 gene was detected in high-calcified than in low-calcified plaques, whereas more remarkable upregulation of the FGFR2 gene was observed in the low-calcified plaques (A). Comparison of signal intensities revealed significant differences between high-calcified (H7-H9) and low-calcified plaques (L7-L9) concerning the protein expression of ANGPTL4 and FGFR2 on Western blotting (B). Abbreviations: ANGPTL4, angiopoietin-like protein 4; FGFR2, fibroblast growth factor receptor 2; HCP, high-calcified plaque; LCP, low-calcified plaque; mRNA, messenger RNA.*

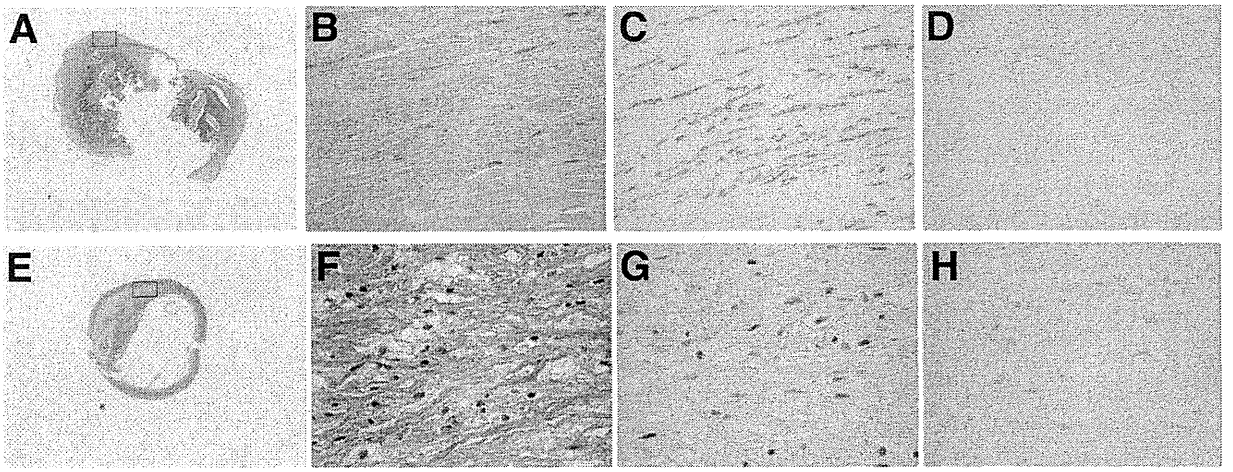

Figure 6. *Representative immunohistochemical study of high-calcified plaques (H7, A-D) and low-calcified plaques (L9, E-H). Hematoxylin–eosin (A, B, E, and F), ANGPTL4 (C), FGFR2 (G), mouse IgG1 (D), and mouse IgG2b (H) staining. (B), (C), (D), (F), (G), and (H) show higher magnifications of the square parts than (A) and (E). Original magnification ×1 (A and E) and ×200 (B, C, D, F, G, and H). Abbreviations: ANGPTL4, angiopoietin-like protein 4; FGFR2, fibroblast growth factor receptor 2; IgG, immunoglobulin G.*

carotid wall, but small number of specimens in the present study and strict criteria for significance of expression might affect the result of analysis.

Conclusions

In high-calcified plaques, ANGPTL4 might be upregulated for antiangiogenic modulating function together with the downregulation of FGFR2, contributing to the stability of the plaques.

References

1. Proudhoot D, Skepper JN, Hegyi L, et al. Apoptosis regulates human vascular calcification by apoptotic bodies. Circ Res 2000;87:1055-1062.
2. Proudhoot D, Davies JD, Skepper JN, et al. Acetylated low-density lipoprotein stimulates human vascular smooth muscle cell calcification by proofing osteoblastic differentiation and inhibition of vascular calcification by apoptotic bodies. Circulation 2002;106: 3044-3050.
3. Ogata T, Yasaka M, Wakugawa Y, et al. Morphological classification of mobile plaques and their association with early recurrence of stroke. Cerebrovasc Dis 2010; 30:606-611.
4. Nandalur KR, Hardie AD, Raghavan P, et al. Composition of the stable carotid plaque. Insights from a multidetector computed tomography study of plaque volume. Stroke 2007;38:935-940.
5. Kwee RM. Systematic review on the association between calcification in carotid plaques and clinical ischemic symptoms. J Vasc Surg 2010;51:1015-1025.
6. Katano H, Yamada K. Analysis of calcium in carotid plaques with Agatston scores for appropriate selection of surgical intervention. Stroke 2007;38:3040-3044.
7. Vemuganti R, Dempsey RJ. Carotid atherosclerotic plaques from symptomatic stroke patients share the molecular fingerprints to develop in a neoplastic fashion: a microarray analysis study. Neuroscience 2005; 131:359-374.
8. Türeyen K, Vemuganti R, Salamat MS, et al. Increased angiogenesis and angiogenic gene expression in carotid artery plaques from symptomatic stroke patients. Neurosurgery 2006;58:971-977.
9. Razuvaev A, Edstrand J, Folkersen L, et al. Correlations between clinical variables and gene-expression profiles in carotid plaque instability. Eur J Vasc Endovasc Surg 2011;42:722-730.
10. Wahlgren C-M, Zheng W, Shaalan W, et al. Human carotid plaque calcification and vulnerability. Cerebrovasc Dis 2009;27:193-200.
11. Lei X, Shi F, Basu K, et al. Proteolytic processing of angiopoietin-like protein 4 by proprotein convertases modulates its inhibitory effects of lipoprotein lipase activity. J Biol Chem 2011;286:15747-15756.
12. Ito Y, Oike Y, Yasunaga K, et al. Inhibition of angiogenesis and vascular leakiness by angiopoietin-related protein 4. Cancer Res 2003;63:6651-6657.
13. Xin X, Yang S, Kowalski J, et al. Peroxisome proliferator-activated receptor gamma ligands are potent target of angiogenesis in vitro and in vivo. J Biol Chem 1999; 274:9116-9119.
14. Turner N, Grose R. Fibroblast growth factor signaling from development to cancer. Nat Rev Cancer 2010; 10:116-129.
15. Yun YR, Won JE, Jeon E, et al. Fibroblast growth factors: biology, function, and application for tissue regeneration. J Tissue Eng 2010;2010:218142.
16. Kadomatsu T, Tabata M, Oike Y. Angiopoietin-like proteins: emerging targets for treatment of obesity and related metabolic diseases. FEBS J 2011;278:559-564.
17. Higashida T, Kanno H, Nakano M, et al. Expression of hypoxia-inducible angiogenic proteins (hypoxia-inducible factor-1α, vascular endothelial growth factor, and E26 transformation-specific-1) and plaque hemorrhage in human carotid atherosclerosis. J Neurosurg 2008; 109:83-91.

18. Saam T, Cai J, Ma L, et al. Comparison of symptomatic and asymptomatic atherosclerotic carotid plaque features with in vivo MR imaging. Radiology 2006; 240:464-472.
19. Altaf N, MacSweeney ST, Gladman J, et al. Carotid intraplaque hemorrhage predicts recurrent symptoms in patients with high-grade carotid stenosis. Stroke 2007; 38:1633-1635.
20. Fisher M, Paganini-Hill A, Martin A, et al. Carotid plaque pathology. Thrombosis, ulceration, and stroke pathogenesis. Stroke 2005;36:253-257.
21. Cai J, Pardali E, Sánchez-Duffhues G, et al. BMP signaling in vascular diseases. FEBS Lett 2012;586:1993-2002.
22. Tanaka K, Matsumoto E, Higashimaki Y, et al. Role of osteoglycin in the linkage between muscle and bone. J Biol Chem 2012;287:11616-11628.